

Nonaheme Cytochrome *c*, a New Physiological Electron Acceptor for [Ni,Fe] Hydrogenase in the Sulfate-Reducing Bacterium *Desulfovibrio desulfuricans* Essex: Primary Sequence, Molecular Parameters, and Redox Properties[†]

Günter Fritz,* Dorrit Griesshaber, Oliver Seth, and Peter M. H. Kroneck

Fachbereich Biologie, Mathematisch-Naturwissenschaftliche Sektion, Universität Konstanz, 78457 Konstanz, Germany

Received June 28, 2000; Revised Manuscript Received November 15, 2000

ABSTRACT: A nonaheme cytochrome *c* was purified to homogeneity from the soluble and the membrane fractions of the sulfate-reducing bacterium *Desulfovibrio desulfuricans* Essex. The gene encoding for the protein was cloned and sequenced. The primary structure of the multiheme protein was highly homologous to that of the nonaheme cytochrome *c* from *D. desulfuricans* ATCC 27774 and to that of the 16-heme HmcA protein from *Desulfovibrio vulgaris* Hildenborough. The analysis of the sequence downstream of the gene encoding for the nonaheme cytochrome *c* from *D. desulfuricans* Essex revealed an open reading frame encoding for an HmcB homologue. This operon structure indicated the presence of an Hmc complex in *D. desulfuricans* Essex, with the nonaheme cytochrome *c* replacing the 16-heme HmcA protein found in *D. vulgaris*. The molecular and spectroscopic parameters of nonaheme cytochrome *c* from *D. desulfuricans* Essex in the oxidized and reduced states were analyzed. Upon reduction, the *pI* of the protein changed significantly from 8.25 to 5.0 when going from the Fe(III) to the Fe(II) state. Such redox-induced changes in *pI* have not been reported for cytochromes thus far; most likely they are the result of a conformational rearrangement of the protein structure, which was confirmed by CD spectroscopy. The reactivity of the nonaheme cytochrome *c* toward [Ni,Fe] hydrogenase was compared with that of the tetraheme cytochrome *c*₃; both the cytochrome *c*₃ and the periplasmic [Ni,Fe] hydrogenase originated from *D. desulfuricans* Essex. The nonaheme protein displayed an affinity and reactivity toward [Ni,Fe] hydrogenase [$K_M = 20.5 \pm 0.9 \mu\text{M}$; $v_{\text{max}} = 660 \pm 20 \text{ nmol of reduced cytochrome min}^{-1} (\text{nmol of hydrogenase})^{-1}$] similar to that of cytochrome *c*₃ [$K_M = 12.6 \pm 0.7 \mu\text{M}$; $v_{\text{max}} = 790 \pm 30 \text{ nmol of reduced cytochrome min}^{-1} (\text{nmol of hydrogenase})^{-1}$]. This shows that nonaheme cytochrome *c* is a competent physiological electron acceptor for [Ni,Fe] hydrogenase.

Anaerobic sulfate-reducing bacteria, such as *Desulfovibrio* sp., can utilize sulfate and dihydrogen as the sole energy source (1). Dihydrogen is oxidized in the periplasmic space by hydrogenase, and the electrons will enter the electron transport chain that contains several low-potential *c*-type cytochromes. A large variety of these *c*-type cytochromes have been isolated from *Desulfovibrio* sp., e.g., the monoheme cytochrome *c*₅₅₃ (M_r 9 kDa) (2) and a family of multiheme *c*-type cytochromes including the tetraheme cytochrome *c*₃ (M_r 14 kDa) (3), the octaheme cytochrome *c*₃ (M_r 26 kDa) (4), the nonaheme cytochrome *c* (M_r 37.5 kDa) (5), and a 16-heme high-molecular-mass cytochrome (Hmc)¹ (M_r 67 kDa) (6). Among these cytochromes, tetraheme cytochrome *c*₃ is the most abundant and structurally best characterized protein (7–16). With the exception of the monoheme cytochrome *c*₅₅₃, which has a methionine and a histidine as axial ligands to iron and a redox potential $E_0' \approx$

$\pm 0 \text{ mV}$, the other multiheme cytochromes show bishistidinyl coordination. These redox proteins cover a broad range of E_0' from 0 to -400 mV (17). The attachment of the heme group by cysteine residues and coordination of the heme iron by histidine residues represents a highly conserved structural motif which is recognized in the primary structure as Cys-X₁-X₂-Cys-His or Cys-X₁-X₂-X₃-X₄-Cys-His.

As sulfate becomes reduced in the cytoplasm, electrons have to be transferred across the cytoplasmic membrane. This problem could be tackled, in principle, after the discovery of the *hmc* operon in *Desulfovibrio vulgaris* Hildenborough (18). The *hmc* operon encodes six proteins (HmcA, -B, -C, -D, -E, -F) which are proposed to be part of a transmembrane electron-transfer complex. This multisubunit complex is assumed to transfer electrons liberated in the periplasm to redox proteins in the cytoplasm (19). HmcA is the 16 heme containing *c*-type cytochrome (Hmc = high-molecular-mass cytochrome) which was isolated from the periplasmic as well as from the membrane fraction of *D. vulgaris* and *Desulfovibrio gigas*. This protein was only slowly reduced by hydrogenase. However, in recent studies it was shown that small amounts of cytochrome *c*₃ increased the reduction rate of HmcA protein and homologous nonaheme cytochrome *c* (ncc) from *Desulfovibrio desulfuricans* ATCC 27774 (DdA) (19, 20). Here we will report on the primary sequence, the

[†] This work was supported by the Deutsche Forschungsgemeinschaft, Volkswagenstiftung, and Fonds der Chemie.

* To whom correspondence should be addressed at Biochemisches Institut, Winterthurer Strasse 190, Universität Zürich, CH-8057 Zürich, Switzerland. Tel: +41-1-635-5554. Fax: +41-1-635-5905. E-mail: gfritz@bioc.unizh.ch.

¹ Abbreviations: DdA, *Desulfovibrio desulfuricans* ATCC 27774; DdE, *Desulfovibrio desulfuricans* Essex; Hmc, high-molecular-mass cytochrome; ncc, nonaheme cytochrome *c*.

biochemical and spectroscopic properties, and the redox behavior of nonaheme cytochrome *c* (*ncc*) from *D. desulfuricans* Essex (*DdE*). From comparative kinetic studies with hydrogenase and tetraheme cytochrome *c*₃ isolated from the same organism, it is concluded that *ncc* directly accepts electrons from hydrogenase in vivo.

MATERIALS AND METHODS

Cell Cultivation and Protein Purification. *D. desulfuricans* Essex was grown on mineral medium containing 30 mM lactate as the electron donor and 15 mM sulfate as the terminal acceptor as described elsewhere (21).

Frozen cells (0.3–0.5 g mL⁻¹ wet weight) were suspended in 10 mM potassium phosphate, pH 7.0, containing a few crystals of DNase II and MgCl₂·6H₂O. Cells were broken by two passages in a French press (138 MPa; Aminco, Urbana, IL). The crude extract was centrifuged for 1 h at 100000g, giving the soluble fraction as the supernatant. The soluble fraction contained both periplasmic and cytoplasmic proteins. The brownish pellet was referred to as the membrane fraction.

All purification steps were performed at 4 °C in the presence of air.

Purification of the Nonaheme Cytochrome *c* from the Soluble Fraction. The soluble fraction was loaded onto a DEAE column (5.0 cm × 6.0 cm, Whatman) equilibrated with 20 mM Tris-HCl, pH 8.0. The fraction passing through the column without binding was loaded onto a hydroxylapatite column (1.6 cm × 12 cm, Calbiochem) equilibrated with 10 mM potassium phosphate buffer, pH 7.0. The column was developed with a linear gradient of 20 mM potassium phosphate buffer and 1.0 M NaCl, pH 7.0. Fractions containing *ncc* were collected, concentrated by ultrafiltration, and loaded onto a Superdex 75 column (1.6 cm × 60 cm, Pharmacia-Amersham) equilibrated in 20 mM potassium phosphate buffer and 150 mM NaCl, pH 7.0. Fractions containing the *ncc* were combined and dialyzed against 10 mM sodium phosphate, pH 7.0, and loaded onto a MonoS column (0.5 cm × 5 cm, Pharmacia-Amersham). The *ncc* was eluted in a linear gradient of 10 mM sodium phosphate and 250 mM NaCl, pH 7.0.

Purification of Nonaheme Cytochrome *c* from the Membrane Fraction. The membrane fraction was washed in 20 mM potassium phosphate, pH 7.0, ultracentrifuged, and solubilized in 100 mM potassium phosphate, pH 7.0, containing 4% (by mass) Triton X-100; the protein:detergent ratio was 1:4 (w/w). After being stirred for 45 min at room temperature, the suspension was centrifuged for 1 h at 100000g, giving the solubilized membrane fraction as the supernatant. The pellet was treated again with Triton X-100 as described above, and both supernatants were combined. The solubilize was dialyzed against 10 mM potassium phosphate buffer, pH 6.0, and loaded on a CM column (5.0 cm × 6.0 cm, Whatman) equilibrated with 10 mM potassium phosphate buffer and 0.05% Triton X-100, pH 6.0. The column was washed with 2–3 volumes of buffer containing Triton X-100 and 4 column volumes of buffer without Triton X-100. The bound cytochromes were eluted in a linear gradient with 20 mM potassium phosphate buffer and 0.5 M NaCl, pH 6.0. The *ncc*-containing fractions were dialyzed against 10 mM potassium phosphate buffer, pH 6.5, and

loaded on a ResourceS column (1.0 cm × 8 cm, Pharmacia-Amersham). The bound *ncc* was eluted in a linear gradient with 20 mM potassium phosphate buffer and 250 mM NaCl, pH 6.5. The *ncc*-containing fractions were concentrated in a ultrafiltration stirring cell (Amicon) and loaded on a Superdex 75 column (1.6 cm × 60 cm, Pharmacia-Amersham), equilibrated in 20 mM potassium phosphate buffer and 150 mM NaCl, pH 7.0, and eluted in the same buffer.

Purification of [Ni,Fe] Hydrogenase. The soluble fraction from the French press cell rupture was dialyzed against 20 mM Tris-HCl, pH 8.0, and loaded on a DEAE column (5.0 cm × 6.0 cm, Whatman) equilibrated with the same buffer. Hydrogenase was eluted with a linear gradient of 20 mM Tris-HCl and 1.0 M NaCl, pH 8.0. Fractions containing hydrogenase were collected and dialyzed against 10 mM Tris-HCl, pH 7.6. The sample was loaded onto a TMAE column (1.6 cm × 12 cm, Merck), which was developed with a linear gradient of 20 mM Tris-HCl and 1.0 M NaCl, pH 7.6. Hydrogenase was collected and concentrated by ultrafiltration. The concentrated sample was loaded onto a Superdex 75 column (1.6 cm × 60 cm, Pharmacia-Amersham), equilibrated in 20 mM potassium phosphate buffer and 100 mM NaCl, pH 7.0, and eluted in the same buffer. Fractions containing hydrogenase were combined, concentrated, and frozen in liquid nitrogen.

Purification of Cytochrome *c*₃. Cytochrome *c*₃ was obtained from the soluble fraction after French press cell treatment. The soluble fraction was loaded onto a DEAE column (5.0 cm × 6.0 cm, Whatman) equilibrated with 20 mM Tris-HCl, pH 8.0. The fraction passing the column was loaded onto a hydroxylapatite column (2.6 cm × 12 cm, Calbiochem) equilibrated with 10 mM potassium phosphate buffer, pH 7.0. The column was developed with a linear gradient of 20 mM potassium phosphate buffer and 1.0 M NaCl, pH 7.0. Fractions containing cytochrome *c*₃ were combined, concentrated by ultrafiltration, loaded on a Superdex 75 column (1.6 cm × 60 cm, Pharmacia-Amersham) equilibrated in 20 mM potassium phosphate buffer and 150 mM NaCl, pH 7.0, and eluted in the same buffer.

Analytical Methods. Protein was determined by the bicinchoninic acid method (22) or by the microbiuret method at 550 nm (23) after TCA/DOC precipitation (24). Bovine serum albumin served as the standard. For determination of nonaheme cytochrome *c*, cytochrome *c*₃ served as a standard.

The native molecular mass was determined by analytical size exclusion chromatography on a Superdex 75 column (1.6 × 60 cm, Pharmacia-Amersham) equilibrated in buffer [50 mM potassium phosphate, 150 mM KCl, and 5% (v/v) glycerol, pH 7.0]. The analysis of the reduced protein was performed in the anaerobe chamber in oxygen-free buffer containing sodium dithionite (1 mM). The column was calibrated with standard proteins (12.4–200 kDa, Sigma).

Reaction of Nonaheme Cytochrome *c* and Cytochrome *c*₃ with [Ni,Fe] Hydrogenase. The reduction of *ncc* and cytochrome *c*₃ by H₂ and reactivated [Ni,Fe] hydrogenase was followed at 552 nm at 25 °C. The reaction mixture contained various concentrations (5–50 μM) of nonaheme protein or cytochrome *c*₃ in 50 mM potassium phosphate, pH 7.5, in a modified Thunberg cuvette, sealed with a rubber septum. Oxygen was removed from the solutions by eight cycles of vacuum and flushing with argon as described elsewhere (25), and the samples were stored in an anaerobe chamber, 95%

N₂ and 5% H₂ (Coy, MI Grass Lake, MI). The hydrogenase was activated by incubation overnight at 8 °C in the anaerobe chamber and diluted in buffer containing 1 mg mL⁻¹ BSA to avoid adsorption on glass and plastic ware. The atmosphere in the cuvette was replaced by hydrogen, ensuring that the solution was hydrogen saturated, and the reaction was started by addition of hydrogenase to a final concentration of 4 nM. The reaction rate ν was expressed as nanomoles of totally reduced cytochrome per minute and per nanomole of hydrogenase. The kinetic parameter k_{cat} was expressed as the number of electrons transferred from hydrogenase to cytochrome per second. To test a possible stimulation of the reduction rates of nonaheme cytochrome *c* by cytochrome *c*₃, we performed assays with nonaheme cytochrome *c* at concentrations of 1.2 and 1.6 μ M and added cytochrome *c*₃ at a concentration range of 0.03–0.16 μ M.

Midpoint Redox Potential of Nonaheme Cytochrome *c*. Potentiometric titrations were performed under anaerobic conditions in a modified Thunberg cuvette as described previously (26). The protein concentration was 2 μ M in 100 mM potassium phosphate, pH 7.0, and redox mediators were added to a final concentration of 6 μ M.

Spectroscopic Methods. Reduction of cytochromes by H₂/[Ni,Fe] hydrogenase was recorded with a Cary 210 spectrophotometer equipped with temperature-controlled cuvette holders. UV–visible spectra were recorded on a Perkin-Elmer Lambda 16 instrument equipped with temperature-controlled cuvette holders. EPR spectra at X-band (9.6 GHz) were recorded on a Bruker ESP300 spectrometer equipped with peripheral equipment and data handling as described elsewhere (27). CD spectra were recorded in 1 mm cuvettes on a Jasco J-715 spectropolarimeter. The cytochromes were reduced with sodium dithionite, and the cuvettes were sealed with silicone oil and a Teflon stopper in order to prevent reoxidation. Only a small excess of dithionite was added, in view of its intense absorption. The CD spectra are expressed as molar ellipticity, Θ , in units of deg dmol⁻¹ cm⁻¹.

PCR Amplification and Sequence Analysis of the Nonaheme Cytochrome *c* from *Desulfovibrio desulfuricans* Essex. Chromosomal DNA was obtained using the Qiagen tissue extraction kit. Primers for PCR were designed using the program PRIME (Wisconsin Package, Genetics Computer Group, Madison, WI). The first set of primers was derived from the N-terminal sequence of *ncc* and the conserved heme binding motif of *c*-type cytochromes Cys-X₁-X₂-Cys-His (primer 1, 5'-GCK ATH GTK ATG TTY CCN GT-3'; primer 2, 5'-ACT TTT GGC ATA TTG C-3'). Taq polymerase was obtained from Qiagen or Sigma, dCTP, dGTP, dATP, and dTTP (dNTP) were obtained from Pharmacia-Amersham, and primers were obtained from Metabion (Munich, FRG). PCR experiments were carried out on a GeneAmp PCR System 9700 (Perkin-Elmer). A typical PCR reaction had a volume of 50 μ L and contained 0.4 μ M each primer, 0.2 mM dNTP, 40 ng of chromosomal DNA as template, buffer according to the manufacturer, and 1–3 units of Taq polymerase. PCR mixtures were heated for 3 min at 94 °C, followed by 30 cycles at 94 °C for 1 min, at a temperature specific to the primers for 1 min, and at 72 °C for 1.5 min, followed by 7 min at 72 °C.

Single Strand Elongation of Known DNA Fragments. In addition to standard PCR techniques employing a forward and a reverse primer, a single strand elongation (28) with

one primer was performed. This new method is designed for the sequencing of chromosomal DNA upstream and downstream of a known DNA segment.

Two forward primers succeeding one another were derived from a known sequence (primer 3, 5'-TGC CAC AAT GTT ACG TCT TCC-3', for 3' elongation; primer 5, 5'-GCG TTT GGC GAT ATT TGT GGC-3', for 5' elongation). A linear amplification with chromosomal DNA as template was performed as follows. Each reaction sample (50 μ L) of a total of six reactions contained 100–150 ng of chromosomal DNA, 0.2 μ M first (upstream) primer, 0.2 mM dNTP, buffer according to the manufacturer, and 2 units of Taq polymerase. After 30 reaction cycles again 2 units of Taq polymerase was added. The reaction proceeded as follows: heating at 94 °C for 3 min, 60 cycles at 94 °C for 1 min, at 55–62 °C for 1 min, and at 72 °C for 1.5 min, followed by 7 min at 72 °C.

The synthesized single strand DNA was purified with the Qiagen PCR purification kit and was obtained in a final volume of 30–50 μ L. The purified amplification product was ligated by T4 RNA ligase to a single strand linker of known sequence (5'-ATG CGA ATT CGG AAG CTT AAG TTA ACG G-3'). To avoid ligation between linker molecules, the linker was phosphorylated on the 5' and 3' ends. Ligation was performed in the presence of DMSO or PEG 4000 overnight at 16 °C, and the ligase was inactivated by incubation at 65 °C for 20 min.

The ligation product served as a template in the second amplification step, using the second primer in forward direction, located downstream from the first primer (primer 4, 5'-TTC CAC AAC AAA CCC GAG AC-3', for 3'-elongation; primer 6, 5'-GTC AAG CGT CAC GAA ATTGC-3', for 5'-elongation). This second primer enhances the specificity of the reaction product. The reverse primer (5'-CCG TTA ACT TAA GCT TCC GAA TTC GC-3') was derived from the linker sequence.

As a last step the *nonaheme* gene was amplified by a set of primers, which were derived from the known sequence, located upstream and downstream of the *nonaheme* gene. This step was performed with Vent (Qiagen) polymerase because of its proofreading function. The resulting fragment was double strand sequenced by GATC GmbH (Konstanz, Germany).

Sequence analysis was performed with the programs available in the Wisconsin Package, Genetics Computer Group. Database search was performed on the BLAST server at the National Center for Biotechnology Information (29–31).

RESULTS AND DISCUSSION

Primary Structure of Nonaheme Cytochrome *c* and Location in the *Hmc* Operon. The complete amino acid sequence of *ncc* from *DdE* as derived from the gene (GenBank accession number AF127653) exhibited an N-terminal extension of 30 amino acids compared to the N-terminal sequences obtained by Edman sequencing of the *ncc* isolated from the membrane and soluble fractions. This extension had a typical sequence signature of a signal peptide of periplasmic or membrane proteins and was most likely cleaved off prior to release of the mature protein to the periplasmic aspect of the membrane. Therefore, we propose that *ncc* is like the

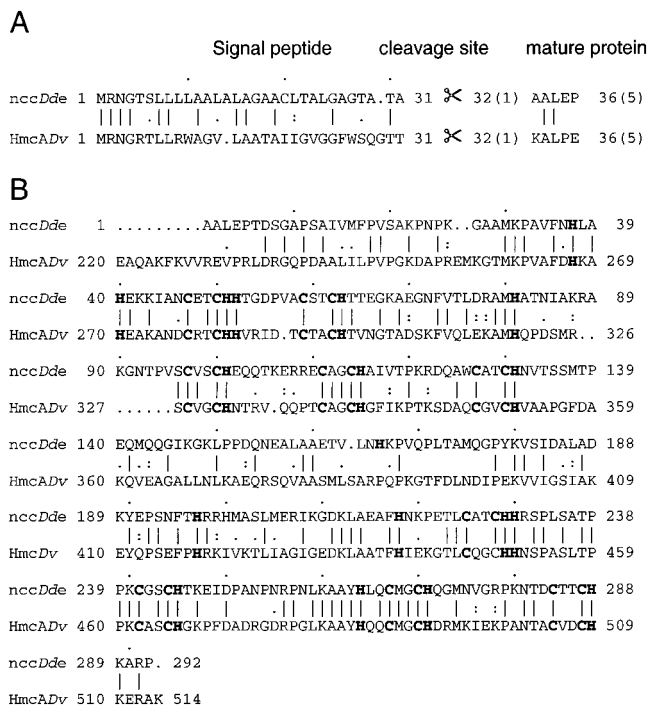


FIGURE 1: Sequence alignment of nonaheme cytochrome *c* of *D. desulfuricans* Essex (nccDdE) with the HmcA protein of *D. vulgaris* Hildenborough (HmcADv) (18). (A) The signal sequences of nonaheme cytochrome *c* and HmcA protein are aligned; both leader peptides have a length of 30 amino acids and have a consensus processing side of T-X₁-X₂-A-L. The numbering of the mature proteins is shown in parentheses. (B) Sequence alignment of the mature nonaheme cytochrome *c* with the C-terminal part of the mature HmcA protein; the heme binding motifs and the conserved histidine residues involved in heme iron coordination are displayed in bold type.

HmcA protein in *D. gigas* and *D. vulgaris* (32, 33), a part of a homologous transmembrane electron-transfer complex in *DdE*, and is located at the periplasmic aspect of the cytoplasmic membrane. After the cells were broken up with the French press, a portion of the protein might have been disrupted from the membrane and thus appeared in the soluble fraction, as observed previously for HmcA protein from *D. vulgaris* and *D. gigas* (32, 33). Ncc from *DdE* showed a high homology to ncc from *DdA* (84% identity) (34, 35) and to the HmcA protein of *D. vulgaris* (18) (43% identity) (Figure 1).

The derived amino acid sequence of mature ncc from *DdE* contained nine binding motifs of the cytochrome *c*-type C-X₁-X₂-C-H, where the cysteine residues are covalently bound to the heme moiety and the imidazole group of the histidine serves as an axial ligand for the heme iron. In addition, nine conserved histidine residues were identified which could serve as the axial ligand for the heme iron. The first five heme binding motifs were clustered in the N-terminal 120 residues. The remaining four motifs were located in the C-terminal part of the protein, separated by a stretch of 90 residues from the first group of motifs. The sequence homology of ncc to tetraheme cytochrome *c*₃ was limited to the arrangement of the heme binding motifs and the motif P-X₁-X₂-F-X₃-H-X₄-X₅-H, which is present in all known sequences of cytochrome *c*₃.

Further sequencing of the PCR product comprising the nonaheme gene revealed the 5' part of a second open reading frame, downstream of the nonaheme gene. This ORF was

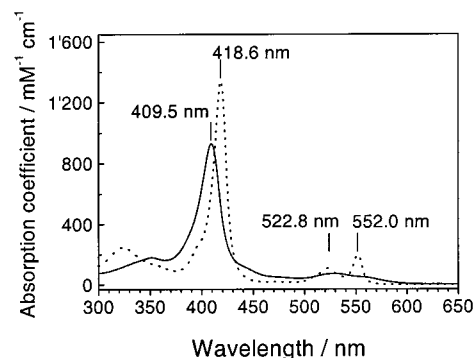


FIGURE 2: UV-visible spectra of nonaheme cytochrome *c* of *D. desulfuricans* Essex: solid line, oxidized protein in 50 mM potassium phosphate and 100 mM NaCl, pH 7.0; dotted line, protein reduced by dihydrogen and catalytic amounts of [Ni,Fe] hydrogenase.

highly homologous (59% identity) to the hmcB gene that is located downstream of hmcA encoding the HmcA protein from *D. vulgaris*.

[Ni,Fe] Hydrogenase and Cytochrome *c*₃. The hydrogenase from *DdE* was pure as judged by SDS-PAGE with two bands at 62 and 30.5 kDa. The native molecular mass was 76 ± 3 kDa according to size exclusion chromatography. In the hydrogen uptake assay with methylene blue as the acceptor, the activity was 220 μmol of H₂ consumed $\text{mg}^{-1} \text{min}^{-1}$ at 37 °C. The hydrogenase was identified as a [Ni,Fe] hydrogenase by EPR spectroscopy (data not shown).

Cytochrome *c*₃ from *DdE* was purified to homogeneity as judged by SDS-PAGE and showed a single band at 14 kDa. The purity index, defined as $(A_{522\text{nm,red}} - A_{570\text{nm,red}})/A_{280\text{nm,ox}}$, was 3.6, which is the highest reported so far.

Biochemical Properties of Nonaheme Cytochrome *c*. Ncc from *DdE* isolated from soluble and membrane fractions showed identical molecular and spectroscopic properties. The yield of ncc from *DdE* (10 mg from the soluble fraction and 8 mg from the membrane fraction, per 100 g of cells) is the highest so far reported for HmcA-like proteins, ranging from less than 1 mg/100 g of cells (32, 36) to 10 mg/100 g of cells (37). These rather high concentrations emphasize the central role of this protein in the metabolism of sulfate-reducing bacteria.

Heme Coordination. The nonaheme protein displayed typical *c*-type cytochrome UV-visible absorption spectra; these were identical for the protein isolated from the membrane or the soluble fractions. The spectra of the oxidized cytochrome showed maxima at 528.8 nm (α/β , 75 $\text{mM}^{-1} \text{cm}^{-1}$), 409.5 nm (γ , 910 $\text{mM}^{-1} \text{cm}^{-1}$), and 351.4 nm (δ , 170 $\text{mM}^{-1} \text{cm}^{-1}$). Second-order derivative spectra revealed further maxima at 441, 472, and 554.6 nm. Reduction with dithionite or hydrogen and hydrogenase led to new absorption maxima at 552 nm (α , 200 $\text{mM}^{-1} \text{cm}^{-1}$), 522.8 nm (β , 120 $\text{mM}^{-1} \text{cm}^{-1}$), 418.6 nm (γ , 1340 $\text{mM}^{-1} \text{cm}^{-1}$), and 323.2 nm (δ , 250 $\text{mM}^{-1} \text{cm}^{-1}$). Second-order derivative spectra revealed shoulders at 532 and 511 nm (Figure 2).

The EPR spectrum of ncc (oxidized, as isolated) showed resonances at $g = 1.51$, 2.26, 2.63, and 2.97, typical for low-spin heme [Fe(III)] centers that are bishistidine coordinated. Additional features around $g = 3.85$ and 4.41 with an absorption-like shape indicated a noncoplanarity of the coordinated imidazole rings (Figure 3). The spectrum

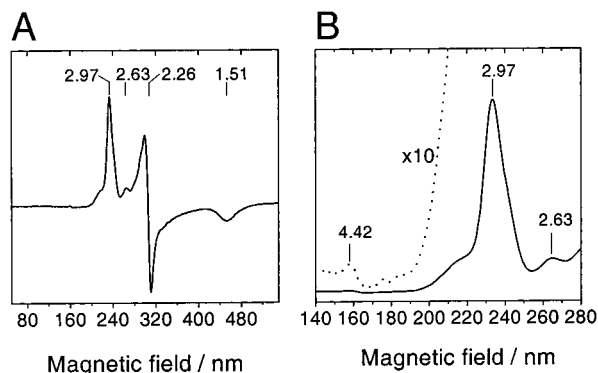


FIGURE 3: EPR spectrum of nonaheme cytochrome *c* of *D. desulfuricans* Essex. Conditions: protein (oxidized), 130 μ M, in 50 mM potassium phosphate and 100 mM NaCl, pH 7.0; modulation amplitude, 1 mT; microwave frequency, 9.65 GHz; microwave power, 2.0 mW; temperature, 10 K. (A) Complete spectrum. (B) Signals at low magnetic field enlarged.

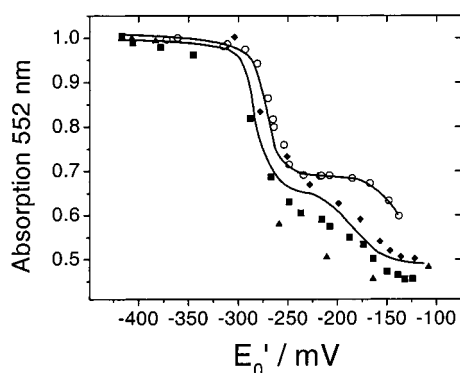


FIGURE 4: Determination of midpoint redox potentials of heme groups in nonaheme cytochrome *c* of *D. desulfuricans* Essex. Open circles represent a reductive titration with dithionite; solid symbols represent oxidative titrations with potassium ferricyanide of heme groups in the nonaheme protein. A strong hysteresis was observed in the oxidative titration for high-potential heme groups.

resembles spectra of other low-spin multiheme proteins carrying low-spin centers with bishistidine coordination, like cytochrome *c*₃ from *Desulfovibrio* sp. (12, 37–39) and *ncc* from *DdA* (40), as well as the HmcA protein from *D. vulgaris* and *D. gigas* (6, 32, 41).

The midpoint redox potentials of the nine heme groups are in a range of –200 to –300 mV (Figure 4), which is narrower than reported for the hemes in HmcA proteins from *D. vulgaris* and *D. gigas* (32, 41).

Reduction by [Ni,Fe] Hydrogenase. The reduction of HmcA protein from *D. vulgaris* sp. by H₂ and hydrogenase was rather slow and increased after addition of a catalytic amount of cytochrome *c*₃ (19); a similar result was reported for *ncc* from *DdA* (5). On the basis of these data, the authors proposed that HmcA protein or *ncc* had to be reduced in vivo by cytochrome *c*₃, mediating electrons from hydrogenase. In contrast, we observed that the *ncc* from *DdE* was reduced by H₂ and hydrogenase at rather high rates. These rates did not increase by the addition of cytochrome *c*₃ from *DdE* up to 10% of the amount of *ncc* in the reduction assay under nonsaturating conditions. The reduction of *ncc* from *DdE* [660 ± 20 nmol min^{–1} (nmol of hydrogenase)^{–1}] occurred at almost the same maximum rate as that of cytochrome *c*₃ from *DdE* [790 ± 30 nmol min^{–1} (nmol of hydrogenase)^{–1}]. In terms of electron transfer the rate of

reduction of *ncc* ($k_{\text{cat}} = 99 \pm 3$ s^{–1}) was even higher than the reduction of cytochrome *c*₃ ($k_{\text{cat}} = 53 \pm 2$ s^{–1}). The maximum reduction rate of *ncc* from *DdE* was about 1700-fold higher than that observed for HmcA protein (19) and about 160-fold higher than for *ncc* from *DdA* (5). Note that in earlier studies the reduction rates of *ncc* from *DdA* were recorded under nonsaturating conditions (5). As a consequence, the reactivity of the cytochromes with hydrogenase was underestimated, and *ncc* was not regarded as a direct physiological electron acceptor. In contrast, the high reduction rates observed in our study represent v_{max} values derived from kinetic studies where the concentration of the cytochromes was varied. From these measurements very similar K_{M} values for *ncc* (20.5 ± 0.9 μ M) and cytochrome *c*₃ (12.6 ± 0.7 μ M) were obtained. These K_{M} values were in the same range as values determined for various cytochromes *c*₃ in previous studies [7.4 μ M (42), 30 μ M (43), 37 μ M (20)]. From our data, we conclude that both *ncc* and cytochrome *c*₃ can act as efficient physiological electron acceptors for [Ni,Fe] hydrogenase in vivo. Further evidence for an alternative electron acceptor of hydrogenase in *D. desulfuricans* came from a recent genetic study (44). In this study the gene encoding cytochrome *c*₃ had been deleted and the mutant strains were still able to grow on hydrogen and sulfate as the sole energy source. Therefore, another redox protein must act as an electron carrier in the electron-transfer chain, and quite obviously, cytochrome *c*₃ is not required as the electron acceptor for hydrogenase in vivo. However, the deletion of the *hmc* operon of *D. vulgaris*, including the gene encoding HmcA which is homologous to *ncc* in *D. desulfuricans*, impairs growth on hydrogen and sulfate (45). This demonstrates the need of HmcA in the transfer of electrons liberated by hydrogen oxidation.

Redox-Dependent Conformational Transition. The apparent molecular weight of *ncc* derived from size exclusion chromatography (43 ± 0.2 kDa; $n = 2$) was higher than the calculated weight of the mature peptide (37.2 kDa, including the nine *c*-type heme groups). Such a deviation is observed for nonglobular proteins with an elliptic shape. The crystal structure of *ncc* from *DdA* (5) and *ncc* from *DdE* [see preceding paper (59)] shows that the molecule has an elliptic rather than a globular shape, in good agreement with our chromatographic data. The reduced protein eluted at an even higher molecular mass of 47 ± 0.2 kDa ($n = 2$), most probably as a result of a redox-dependent conformational change.

This redox-dependent conformational transition was confirmed by CD spectroscopy. The CD spectra of *ncc* and cytochrome *c*₃ revealed changes in the UV and visible regions upon reduction with dithionite (Figure 5). The bands in the visible region between 350 and 450 nm originate from the heme moieties, whereas the bands in the UV region between 190 and 240 nm result from electronic transitions of the protein backbone and reflect the secondary structure of the protein (46). Both proteins showed in the Fe(III) state positive signals in the visible region, with maxima located at the maxima of the corresponding absorption bands at 409 nm. In the Fe(II) state both cytochromes displayed derivative-like CD signals. The crossover points at 422 and 424 nm were slightly red shifted compared to the corresponding absorption maxima at 419 nm. In the case of *ncc*, the change in the CD spectrum upon reduction was more pronounced

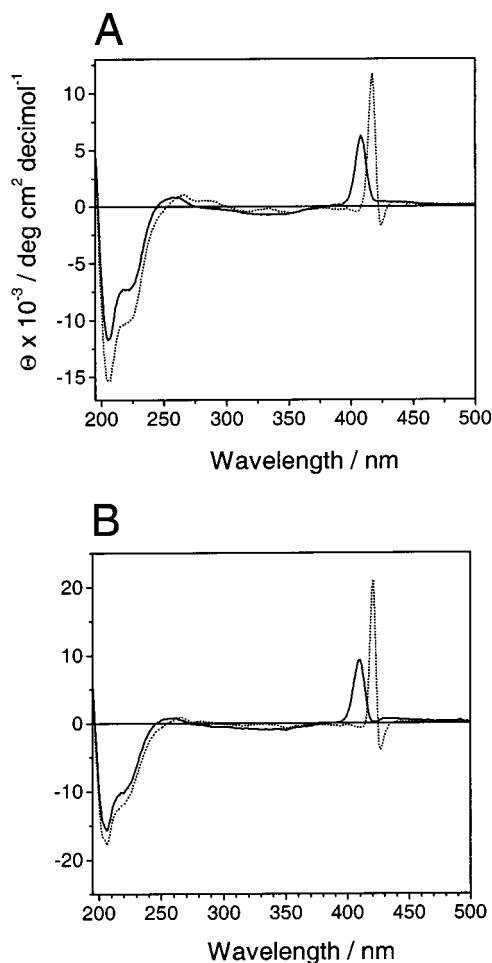


FIGURE 5: CD spectra of oxidized and reduced nonaheme cytochrome *c* (A) and oxidized and reduced cytochrome *c*₃ (B), both from *D. desulfuricans* Essex in 20 mM potassium phosphate, pH 7.0.

than in cytochrome *c*₃. The changes in the UV region corresponded to a 40% increase in intensity of the CD bands in the reduced state compared to those in the oxidized state. It is noteworthy that similar redox-induced changes in the CD spectrum were also detected for cytochrome *c*₃, but to a much lower degree. Consistent with this observation, the structures of oxidized and reduced cytochrome *c*₃ from *Desulfovibrio africanus* (15) and *D. gigas* (16) differed only slightly. Furthermore, *ncc* appeared more sensitive to changes in pH in the reduced state than in the oxidized state. In the oxidized state the protein was almost insensitive to pH changes over the range 4–10. In contrast, *ncc* in the reduced state revealed major changes in the CD spectra upon changes in pH. When the pH was increased, the intensity of the bands in the UV region decreased; furthermore, the line width of the bands in the visible region decreased, resulting in more intensive bands (Figure 6).

The redox-dependent conformational transition of *ncc* from *DdE* was also reflected in a significant change of its *pI* as determined by chromatofocusing. A redox-induced uptake and release of protons, the so-called redox–Bohr effect, was examined in great detail for cytochrome *c*₃ (47–51). Hereby, reduction of the heme groups in cytochrome *c*₃ triggered the capture of two protons which were released upon reoxidation. Such an uptake of protons triggered by the reduction of the cytochrome *c*₃ corresponds to an increase in *pI*. In contrast,

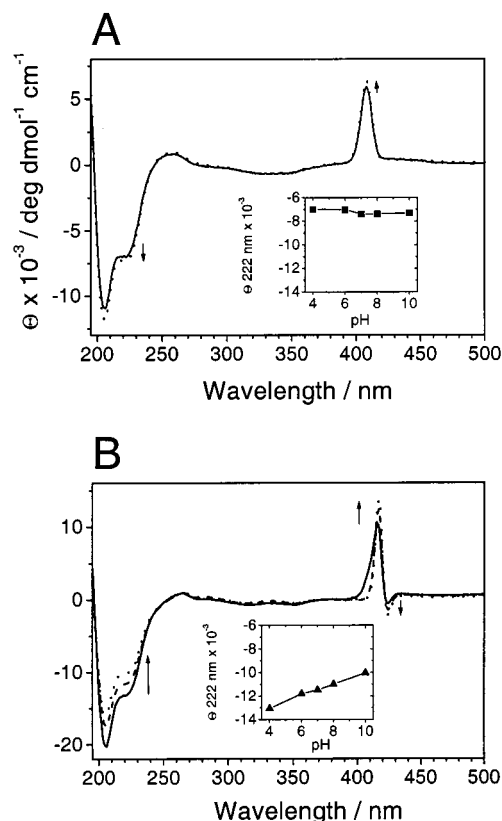


FIGURE 6: pH dependence of the CD spectra of nonaheme cytochrome *c*. The insets show the change of the band at 222 nm with increasing pH (A) The spectra of oxidized nonaheme cytochrome *c* at pH 4 (solid line) and pH 10 (dotted line) are shown. (B) The spectra of reduced nonaheme cytochrome *c* at pH 4 (solid line), pH 7 (dashed line), and pH 10 (dotted line) are shown. Arrows in panels A and B indicate the changes of the spectra with increasing pH.

the *pI* of *ncc* and cytochrome *c*₃ from *DdE* decreased upon reduction; i.e., protons became liberated. Again, the effect was enormous in the case of *ncc* where the *pI* dropped from 8.25 in the oxidized state to 5.0 in the reduced state. In comparison, the *pI* of cytochrome *c*₃ shifted only slightly from 8.95 to 8.25 upon reduction. Therefore, it is concluded that the reduction-induced decrease in *pI* of *ncc* is not due to a redox–Bohr effect. For more detailed analysis of this phenomenon, the *pI* of the oxidized *ncc* was calculated (52, 53) on the basis of the crystal structure (59). Hereby, nine propionate residues of the heme groups were included that are accessible to the solvent; contributions from cysteine residues forming the thioether bridges to the heme groups were neglected. A *pI* of 7.9 was calculated, in good agreement with the observed value of 8.25. The drop of the *pI* to 5.0 upon reduction could only be explained by a rather drastic change in *pK*_a of a few distinct residues. We propose that the redox-induced conformational change observed by CD spectroscopy and size exclusion chromatography altered the solvent accessibility and *pK*_a of several acidic residues which will form a negative patch at the protein surface.

It is suggested that the redox-dependent change in *pK*_a of residues in periplasmic multi-heme cytochromes not only is important for energetic reasons as proposed by Xavier and co-workers (47–51, 54), but also plays an important role in the recognition of electron-transfer partners. Electron transfer itself is very fast, and the energetics of the reaction are

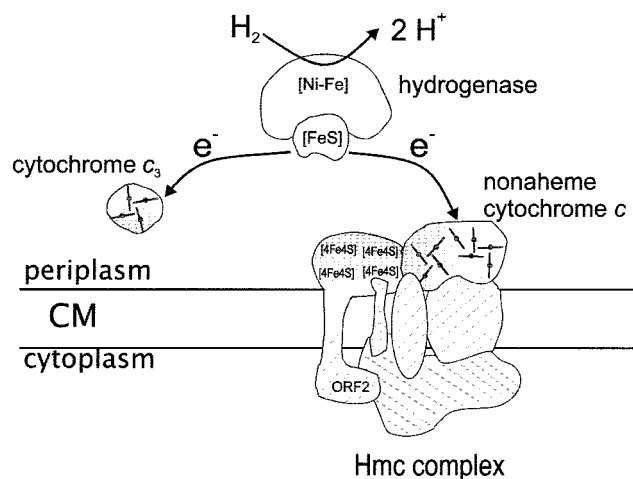


FIGURE 7: Model for the Hmc complex in *D. desulfuricans* Essex and schematic electron flow. The redox components found in *D. desulfuricans* are indicated in gray. The subunits that are encoded in the *hmc* operon of *D. vulgaris* Hildenborough (18) are hatched.

controlled by the redox potential. The recognition and binding between redox proteins is therefore essential since it represents an effective way to direct the kinetics of the reaction (55–57). Protein–protein interaction and recognition is mediated by specific patches in form and charge of the surface. Variation of the charge of the cytochrome surface leads to a different recognition pattern. Consequently, the reduced protein may no longer be able to interact with the electron-donating hydrogenase until the electrons are delivered to the electron-accepting redox partner in the membrane-bound Hmc complex (Figure 7).

The reason for the existence of multiple heme prosthetic groups in the *ncc* or the Hmc cytochrome is not well understood. Matias et al. (5) proposed that the *ncc* from *DdA* spans the cytoplasmic membrane, suggesting that the multiple heme groups are required for transmembrane electron transfer. This model appears not very likely, since nonaheme cytochromes *c* from neither *DdA* nor *DdE* comprise transmembrane helices or hydrophobic surfaces and will therefore not be able to integrate into the lipophilic membrane. Transmembrane electron transfer most likely proceeds via *b*-type cytochromes that are indeed found in the cytoplasmic membrane of *Desulfovibrio* sp. (58), where they are part of the Hmc complex, as proposed from sequence data (18). In contrast, the multiheme *c*-type cytochromes (nonaheme, Hmc) in *Desulfovibrio* sp. probably function as periplasmic electron funnels or reservoirs in order to optimize the electron flux from the periplasmic to the cytoplasmic compartment of the bacterial cell.

REFERENCES

- Thauer, R. K., Jungermann, K., and Decker, K. (1977) *Bacteriol. Rev.* 41, 100–180.
- Blackledge, M. J., Medvedeva, S., Ooncin, M., Guerlesquin, F., Bruschi, M., and Marion, D. (1995) *J. Mol. Biol.* 245, 661–681.
- Der Vartanian, D. V., and LeGall, J. (1974) *Biochim. Biophys. Acta* 346, 79–99.
- Haladjian, J., Bianco, P., Guerlesquin, F., and Bruschi, M. (1991) *Biochem. Biophys. Res. Commun.* 179, 605–610.
- Matias, P., Coelho, R., Pereira, I. A. C., Coelho, A. V., Thompson, A. W., Sieker, L. C., LeGall, J., and Carrondo, M. A. (1999) *Structure* 7, 119–130.
- Bruschi, M., Bertrand, P., More, C., Leroy, G., Bonicel, J., Haladjian, J., Chottard, G., Pollock, W. B., and Voordouw, G. (1992) *Biochemistry* 31, 3281–3288.
- Haser, R., Pierrot, M., Frey, M., Payan, F., Astier, J. P., Bruschi, M., and Le Gall, J. (1979) *Nature* 282, 806–810.
- Pierrot, M., Haser, R., Frey, M., Payan, F., and Astier, J. P. (1982) *J. Biol. Chem.* 257, 14341–14348.
- Higuchi, Y., Kusunoki, M., Matsuura, Y., Yasuoka, N., and Kakudo, M. (1984) *J. Mol. Biol.* 172, 109–139.
- Matias, P. M., Frazão, C., Morais, J., Coll, M., and Carrondo, M. A. (1993) *J. Mol. Biol.* 234, 680–699.
- Czjzek, M., Payan, F., Guerlesquin, F., Bruschi, M., and Haser, R. (1994) *J. Mol. Biol.* 243, 653–667.
- Morais, J., Palma, P. N., Frazão, C., Caldeira, J., LeGall, J., Moura, I., Moura, J. J. G., and Carrondo, M. A. (1995) *Biochemistry* 34, 12830–12841.
- Matias, P. M., Morais, J., Coelho, R., Carrondo, M. A., Wilson, K., Dauter, Z., and Sieker, L. (1996) *Protein Sci.* 5, 1342–1354.
- Messias, A. C., Kastrau, D. H., Costa, H. S., LeGall, J., Turner, D. L., Santos, H., and Xavier, A. V. (1998) *J. Mol. Biol.* 281, 719–739.
- Nørager, S., Legrand, P., Pieulee, L., Hatchikian, C., and Roth, M. (1999) *J. Mol. Biol.* 290, 881–902.
- Brennan, L., Turner, D. L., Messias, A. C., Teodoro, M. L., LeGall, J., Santos, H., and Xavier, A. V. (2000) *J. Mol. Biol.* 298, 61–82.
- Moura, J. J. G., Costa, C., Liu, M.-Y., Moura, I., and LeGall, J. (1991) *Biochim. Biophys. Acta* 1058, 61–66.
- Rossi, M., Pollock, W. B. R., Reij, M. W., Keon, R. G., Fu, R., and Voordouw, G. (1993) *J. Bacteriol.* 175, 4699–4711.
- Pereira, I. A. C., Romão, C. V., Xavier, A. V., LeGall, J., and Teixeira, M. (1998) *JBIC, J. Biol. Inorg. Chem.* 3, 494–498.
- Aubert, C., Brugna, M., Dolla, A., Bruschi, M., and Giudici-Ortoni, M.-T. (2000) *Biochim. Biophys. Acta* 1476, 85–92.
- Steuber, J., Arendsen, A. F., Hagen, W. R., and Kroneck, P. M. (1995) *Eur. J. Biochem.* 233, 873–879.
- Smith, P. K., Krohn, R. I., Hermanson, G. T., Mallia, A. K., Gartner, F. H., Provenzano, M. D., Fujimoto, E. K., Goeke, N. M., Olson, B. J., and Klenk, D. C. (1985) *Anal. Biochem.* 150, 76–85.
- Goa, J. (1953) *Scand. J. Clin. Lab. Invest.* 5, 219–222.
- Bensadoun, A., and Weinstein, D. (1976) *Anal. Biochem.* 70, 241–50.
- Beinert, H., Orme-Johnson, W. H., and Palmer, G. (1978) *Methods Enzymol.* 54, 111–132.
- Dutton, P. L. (1978) *Methods Enzymol.* 54, 411–435.
- Neese, F., Zumft, W. G., Antholine, W. E., and Kroneck, P. M. H. (1996) *J. Am. Chem. Soc.* 118, 8692–8699.
- Seth, O. (1999) Ph.D. Thesis, Universität Konstanz, Konstanz.
- Altschul, S. F., Gish, W., Miller, W., Myers, E. W., and Lipman, D. J. (1990) *J. Mol. Biol.* 215, 403–410.
- Madden, T. L., Tatusov, R. L., and Zhang, J. (1996) *Methods Enzymol.* 266, 131–141.
- Zhang, J., and Madden, T. L. (1997) *Genome Res.* 7, 649–656.
- Chen, L., Pereira, M. M., Teixeira, M., Xavier, A. V., and LeGall, J. (1994) *FEBS Lett.* 347, 295–299.
- Pereira, I. A. C., Romão, C. V., LeGall, J., Xavier, A. V., and Teixeira, M. (1997) *JBIC, J. Biol. Inorg. Chem.* 2, 23–31.
- Matias, P. M., Saraiva, L. M., Soares, C. M., Coelho, A. V., LeGall, J., and Carrondo, M. A. (1999) *JBIC, J. Biol. Inorg. Chem.* 4, 478–494.
- Saraiva, L. M., da Costa, P. N., and LeGall, J. (1999) *Biochem. Biophys. Res. Commun.* 262, 629–634.
- Higuchi, Y., Inaka, K., Yasuoka, N., and Yagi, T. (1987) *Biochim. Biophys. Acta* 911, 341–348.
- Pollock, W. B. R., Loutfi, M., Bruschi, M., Rapp-Giles, B. J., Wall, J. D., and Voordouw, G. (1991) *J. Bacteriol.* 173, 220–228.
- Park, J. S., Kano, K., Niki, K., and Akutsu, H. (1991) *FEBS Lett.* 285, 149–151.

39. Magro, V., Pieulle, L., Forget, N., Guigliarelli, B., Petillot, Y., and Hatchikian, E. C. (1997) *Biochim. Biophys. Acta* 1342, 149–163.
40. Coelho, A. V., Matias, P. M., Sieker, L. C., Morais, J., Carrondo, M. A., Lampreia, J., Costa, C., Moura, J. J. G., Moura, I., and LeGall, J. (1996) *Acta Crystallogr. D* 52, 1202–1208.
41. Verhagen, M. F., Pierik, A. J., Wolbert, R. B., Mallee, L. F., Voorhorst, W. G., and Hagen, W. R. (1994) *Eur. J. Biochem.* 225, 311–319.
42. Nivière, V., Hatchikian, E. C., Bianco, P., and Haladjian, J. (1988) *Biochim. Biophys. Acta* 935, 34–40.
43. Brugna, M., Giudici-Orticoni, M. T., Spinelli, S., Brown, K., Tegoni, M., and Bruschi, M. (1998) *Proteins* 33, 590–600.
44. Rapp-Giles, B. J., Casalot, L., English, R. S., Ringbauer, J. J., Dolla, A., and Wall, J. D. (2000) *Appl. Environ. Microbiol.* 66, 671–677.
45. Dolla, A., Pohorelic, B., Voordouw, J., and Voordouw, G. (2000) *Arch. Microbiol.* 174, 143–151.
46. Pelton, J. T., and McLean, L. R. (2000) *Anal. Biochem.* 277, 167–176.
47. Xavier, A. V., Moura, J. J. G., LeGall, J., and DerVartanian, D. V. (1979) *Biochimie* 61, 689–695.
48. Santos, H., Moura, J. J. G., Moura, I., LeGall, J., and Xavier, A. V. (1984) *Eur. J. Biochem.* 141, 283–296.
49. Coletta, M., Catarino, T., LeGall, J., and Xavier, A. V. (1991) *Eur. J. Biochem.* 202, 1101–1106.
50. Turner, D. L., Salgueiro, C. A., Catarino, T., LeGall, J., and Xavier, A. V. (1994) *Biochim. Biophys. Acta* 1187, 232–235.
51. Turner, D. L., Salgueiro, C. A., Catarino, T., LeGall, J., and Xavier, A. V. (1996) *Eur. J. Biochem.* 241, 723–731.
52. Creighton, T. E. (1993) *Proteins—Structures and Molecular Properties*, 2nd ed., Freeman, New York.
53. Hennig, L. (1999) *BioTechniques* 26, 1170–1172.
54. Teixeira, M., Moura, I., Xavier, A. V., Moura, J. J. G., LeGall, J., DerVartanian, D. V., Peck, H. D., Jr., and Huynh, B. H. (1989) *J. Biol. Chem.* 264, 16435–16450.
55. Chen, L., Durley, R., Mathews, F., and Davidson, V. (1994) *Science* 264, 86–90.
56. Zhu, Z., Cunane, L., Chen, Z., Durley, R., Mathews, F., and Davidson, V. (1998) *Biochemistry* 37, 17128–17136.
57. Davidson, V. L. (2000) *Acc. Chem. Res.* 33, 87–93.
58. Odom, J. M., and Peck, H. D., Jr. (1981) *J. Bacteriol.* 147, 161–169.
59. Umhau, S., Fritz, G., Diederichs, K., Breed, J., Welte, W., and Kroneck, P. M. H. (2001) *Biochemistry* 40, 1308–1316.

BI001480+